

Oxidative Damage Is Increased in Human Liver Tissue Adjacent to Hepatocellular Carcinoma

Christoph Jünger,^{1,2*} Bin Cheng,^{1*} Ralph Gehrke,² Volker Schmitz,¹ Hans Dieter Nischalke,¹ Jan Ramakers,¹ Peter Schramel,³ Peter Schirmacher,⁴ Tilman Sauerbruch,¹ and Wolfgang Helmut Caselmann¹

Accumulation of genetic alterations in hepatocarcinogenesis is closely associated with chronic inflammatory liver disease. 8-oxo-2'-deoxyguanosine (8-oxo-dG), the major pro-mutagenic DNA adduct caused by reactive oxygen species (ROS), leads to G:C → T:A transversions. These lesions can be enzymatically repaired mainly by human MutT homolog 1 (hMTH1), human 8-oxo-guanine DNA glycosylase (hOGG1) and human MutY homolog (hMYH). The aim of this study was to evaluate the extent of oxidative damage and its dependence on the cellular antioxidative capacity and the expression of specific DNA repair enzymes in tumor (tu) and corresponding adjacent nontumor (ntu) liver tissue of 23 patients with histologically confirmed hepatocellular carcinoma. 8-oxo-dG levels, as detected by high-pressure liquid chromatography with electrochemical detection, were significantly ($P = .003$) elevated in ntu tissue (median, 129 fmol/ μ g DNA) as compared to tu tissue (median, 52 fmol/ μ g DNA), and were closely associated with inflammatory infiltration. In ntu tissue, the hepatic iron concentration and malondialdehyde levels were significantly ($P = .001$) higher as compared to tu tissue. Glutathione content, glutathione peroxidase activity and manganese superoxide dismutase messenger RNA (mRNA) expression did not show statistical differences between ntu and tu tissue. Real-time reverse transcription polymerase chain reaction revealed in tu tissue significantly ($P = .014$) higher hMTH1 mRNA expression compared to ntu tissue. In contrast, hMYH mRNA expression was significantly ($P < .05$) higher in ntu tissue. No difference in hOGG1 mRNA expression was seen between tu and ntu. **In conclusion**, these data suggest that ROS generated by chronic inflammation contribute to human hepatocarcinogenesis. The role of DNA repair enzymes appears to be of reactive rather than causative manner. (HEPATOLOGY 2004;39:1663–1672.)

Abbreviations: HCV, hepatitis C virus; HCC, hepatocellular carcinoma; ROS, reactive oxygen species; 8-oxo-dG, 8-oxo-2'-deoxyguanosine; MDA, malondialdehyde; GSH, glutathione; GSH-Px, glutathione peroxidase; MnSOD, manganese superoxide dismutase; hMTH1, human MutT homolog 1; hOGG1, human 8-oxo-guanine DNA glycosylase; hMYH, human MutY homolog; mRNA, messenger RNA; tu, tumor; ntu, nontumor; PCR, polymerase chain reaction.

From the ¹Department of Internal Medicine I, University of Bonn, Bonn, Germany; the ²Department of Virus Research, Max-Planck-Institut für Biochemie, Martinsried, Germany; the ³GSF-National Research Center for Environment and Health Institute of Ecological Chemistry, Neuherberg, Germany; and the ⁴Institute of Pathology, University of Cologne, Cologne, Germany.

Received September 10, 2003; accepted March 12, 2004.

*C. J. and B. C. contributed equally to this study.

Supported, in part, by a research grant of the Bonfor Research Council of the University of Bonn (107/38) to W.H.C.

Address reprint requests to: Wolfgang Helmut Caselmann, M.D., Bavarian State Ministry of the Environment, Public Health and Consumer Protection, Rosenkavalierplatz 2, D-81925 München, E-mail: wolfgang.caselmann@stmugv.bayern.de; fax: 49 89 9214 2384.

Copyright © 2004 by the American Association for the Study of Liver Diseases. Published online in Wiley InterScience (www.interscience.wiley.com).

DOI 10.1002/hep.20241

Epidemiological studies have demonstrated a striking correlation between chronic inflammatory liver diseases such as hepatitis B virus or hepatitis C virus (HCV) infection and the occurrence of hepatocellular carcinoma (HCC). Hepatocarcinogenesis is a multistep process that involves the accumulation of both genetic and epigenetic events such as point mutations, gross chromosomal rearrangements, oncogene activation, and tumor suppressor gene inactivation.¹ Reactive oxygen species (ROS) have been implicated in the pathogenesis of degenerative and inflammatory diseases, aging, and cancer.² In liver disease, infiltration of activated phagocytic cells provides an additional source of ROS production that promotes oxidative stress and damage to proteins, lipids, and DNA.³ 8-oxo-2'-deoxyguanosine (8-oxo-dG), one of the major and most deleterious DNA base lesions, is induced by the attack of either hydroxyl radical or singlet oxygen on deoxyguanosine.⁴ 8-oxo-dG is a pro-mutagenic lesion as it mispairs preferentially with adenine

during replication; if DNA repair mechanisms are ineffective, the result is G:C → T:A transversions both *in vitro* and *in vivo*.⁵

“Free” iron catalyzes the formation of ROS and, thereby, the induction of oxidative damage *in vitro*.⁶ *In vivo*, iron is predominantly bound to proteins, minimizing the amount of “free” catalytic iron. However, increased amounts of circulating “free” iron complexes have been reported in conditions of chronic iron overload.⁷ ROS react with polyunsaturated fatty acids to induce the release of toxic and reactive aldehyde metabolites such as malondialdehyde (MDA).⁸ Hepatic lipid peroxidation has been found in various forms of chronic liver disease⁹ and is a proposed driving force for hepatocarcinogenesis in genetic hemochromatosis. Cells are protected against ROS by nonenzymatic antioxidants, predominantly glutathione (GSH), and scavenger enzymes such as glutathione peroxidase (GSH-Px) and manganese superoxide dismutase (MnSOD). An imbalance between the production and detoxification of ROS results in oxidative stress of hepatocytes and favors the induction of DNA mutation.^{3,10}

When cellular DNA damage is detected, the *p53* tumor suppressor gene induces cell cycle arrest to inhibit replicative DNA synthesis.¹¹ A newly emerging role of the *p53* protein is the regulation of DNA excision repair.¹² A specific DNA repair system that comprises the enzymes MutT, MutM, and MutY exists in *Escherichia coli* and prevents 8-oxo-dG–induced mutagenesis. Human homologs of MutT (human MutT homolog 1 [hMTH1]),¹³ MutM (human 8-oxo-guanine DNA glycosylase [hOGG1]),¹⁴ and MutY (human MutY homolog [hMYH])¹⁵ have been characterized. The hMTH1 protein is an 8-oxo-dGTPase that prevents incorporation of 8-oxo-dGTP into nascent DNA by hydrolyzing 8-oxo-dGTP to 8-oxo-dGMP, thereby eliminating 8-oxo-dGTP from the nucleotide precursor pool.¹³ The DNA glycosylase/lyase hOGG1 removes the oxidized base from 8-oxo-dG:C base pairs,¹⁴ while hMYH DNA glycosylase excises misincorporated adenine from 8-oxo-dG:A base pairs formed during DNA replication.¹⁵ Aberrant enzyme expression and gene mutations have been described in several types of cancer^{16–20}; however, to date, expression of *hMTH*, *hOGG1*, and *hMYH* genes has not been investigated in human HCC.

Therefore, the aims of our study were to (1) determine oxidative damage of DNA and lipids in tumor (tu) and corresponding adjacent nontumor (ntu) liver tissue of 23 patients with histologically proven HCC; (2) evaluate the capacity of the cellular antioxidative system in these tissues; and (3) assess the expression of specific DNA repair

enzymes in these tissues to elucidate their potential as contributors to human hepatocarcinogenesis.

Materials and Methods

Patients. Tu and ntu liver tissue was obtained from 23 patients with histologically confirmed HCC after informed consent was given. The ntu liver tissue was at least 1 cm in distance from the tu margin. The median age was 59 years (range, 42 to 71 years). Sixteen patients were male (69.6%) and 7 were female (30.4%). Eight (34.8%) patients showed markers of hepatitis B virus infection, 6 (26.1%) were seropositive for anti-HCV antibodies, and 7 (30.7%) had a history of alcohol abuse. In 2 cases, the underlying cause of liver disease remained unknown. All patients underwent surgical resection or transplantation without prior chemotherapeutic treatment. The tu and corresponding ntu liver tissues were dissected immediately after surgical removal, snap-frozen in liquid nitrogen, and stored at -80°C . The study was performed according to the guidelines of the local ethical committee.

Histopathological Evaluation. Histopathological analyses were performed without knowledge of clinical data. Inflammatory infiltration of ntu liver tissue was graded as absent or minimal, mild, moderate, and severe.²¹

Isolation and Hydrolysis of Hepatic DNA. DNA was isolated using 1 mL 1% sodium dodecyl sulfate, 1 mmol/L ethylenediaminetetraacetic acid and 0.1 mmol/L deferoxamine mesylate (Sigma, Taufkirchen, Germany) to avoid iron catalyzed DNA oxidation.²² Samples were digested with proteinase K (Boehringer Mannheim, Mannheim, Germany) (100 $\mu\text{g}/\text{mL}$) at 50°C for 2 hours. Extracted DNA was dissolved in 20 mmol/L sodium acetate (pH 5.0)/0.1 mmol/L deferoxamine mesylate and denatured at 95°C for 10 minutes. After digestion with 20 μg nuclease P1 (Boehringer Mannheim) at 65°C for 10 min, 1 mol/L Tris/ H_3PO_4 (Sigma) (pH 8.5) was added (10% vol/vol) and samples were hydrolysed with 4 units of calf intestine alkaline phosphatase (Boehringer Mannheim) at 37°C for 60 minutes and filtered through a 5.000 Da cut-off filtration system (Millipore, Bedford, MA).

Analysis of 8-oxo-dG. DNA hydrolysates were separated by high-pressure liquid chromatography (Pharmacia Smart System, Erlangen, Germany) using a RP-18 column (250 \times 4mm; 5 μm ; Merck, Darmstadt, Germany) and 12% methanol (vol/vol) in 50 mmol/L KH_2PO_4 (pH 5.5) as the mobile phase with a flow rate of 600 $\mu\text{L}/\text{min}$. 8-oxo-dG was determined by electrochemical detection (Waters 460 EC-Detector, Waters, Milford, MA) with an oxidation potential of +0.55 V. Deoxyguanosine was measured simultaneously by UV absorbance (Pharmacia μpeak UV-detector) at 260 nm.²²

Determination of Malondialdehyde and Protein Content. Liver tissue was homogenized (10% wt/vol) in ice-cold 1X phosphate-buffered saline (pH 7.4) using 2,6-Di-*tert*-butyl-4-methylphenol (Sigma) to avoid autoxidation and subsequently heated to 90°C for 60 minutes. High-pressure liquid chromatography (Shimadzu, Kyoto, Japan) was used to separate 0.05 mL of the neutralized preparation using an RP-18 column (250×4mm; 10 μm; Merck) and a mixture of 40% methanol and 60% 50 mmol/L potassium phosphate buffer (pH 6.8) as a mobile phase; the flow rate was 1 mL/min. Malondialdehyde-thiobarbituric acid adducts were detected fluorimetrically (Kontron SFM-23, Zürich, Switzerland) at 550 nm using an excitation wavelength of 525 nm.²³ Protein content was determined using the Bio-Rad protein assay (Bio-Rad Laboratories, München, Germany).

Hepatic Iron Determination. Hepatic iron concentration was measured after incineration of the tissue samples by inductively coupled plasma emission spectroscopy using a JY 70 spectrometer (Jobin Yvon, Grasbrunn, Germany) as previously described, with minor modifications.²⁴

Glutathione Assay. Reduced GSH was assayed according to the method of Sedlak and Lindsay.²⁵

Glutathione Peroxidase Assay. The activity of selenium-dependent GSH-Px was assayed as described previously²⁶ with minor modification using hydrogen peroxide as the substrate.

Immunohistochemistry. Cryosections (6 μm thick) were stained by an indirect immunoperoxidase technique using the primary monoclonal mouse antibody DO-7 (DAKO, Glostrup, Denmark).²⁷ This antibody reacts with both wild-type and mutant p53 protein.

RNA Preparation and Reverse Transcription. Total RNA was extracted with the Trizol reagent (Life Technologies, Karlsruhe, Germany). First-strand complementary DNA was prepared from 2 μg total RNA by random priming using Moloney murine leukemia virus reverse transcriptase (Promega, Mannheim, Germany) at 42°C for 60 minutes.

Polymerase Chain Reaction (PCR) Primers and Standard Preparation. External DNA standards were generated by PCR amplification of hepatocellular complementary DNA using the respective oligonucleotide primers (Gibco BRL, Eggenstein, Germany), shown in Table 1, and subsequently purified with the GenElute PCR DNA Purification Kit (Sigma). The concentration was detected spectrophotometrically and diluted to 1 ng/μL with double-distilled (dd) H₂O. Serial dilutions were used to obtain standard curves.

Real-time PCR. *hMTH1*, *hOGG1*, *hMYH alfa* (*hMYHα*), *MnSOD*, and *beta-actin* (*β-actin*) mRNA ex-

Table 1. Oligonucleotide Primers Used for PCR Amplification

Gene	Sequences	GenBank Accession No.	Base No.
<i>hMYHα</i>	5'-GAG GAG CCT CTA GAA CTA TGA-3'	AB032922*	1-19
	5'-AGG CTG TGA CTT CAG CTA C-3'	AB032923†	378-351*
<i>hOGG1</i>	5'-ACA CTG GAG TGG TGT ACT AGC G-3'	AB000410	427-448
	5'-GCG ATG TTG TTG TTG GAG G-3'		726-708
<i>hMTH1</i>	5'-AGC CTC AGC GAG TTC TCC TG-3'	AK026631	138-157
	5'-GAT CTG GCC CAC CTT GTG C-3'		307-291
<i>MnSOD</i>	5'-GAG ATG TTA CAG CCC AGA TAG C-3'	Y00472	293-314
	5'-AAT CCC CAG CAG TGG AAT AAG G-3'		612-591
<i>β-actin</i>	5'-CGG GAA ATC GTG CGT GAC AT-3'	NM001101	689-708
	5'-GAA CTT TGG GGG ATG CTC GC-3'		1400-1381

*Subtype *hMYHα3*

†Subtype *hMYHα4*

pression was measured by real-time PCR using the LightCycler system (Roche Diagnostics, Mannheim, Germany). A standard PCR reaction contained 0.5 μL of each primer (5 μmol/L), 1 μL magnesium chloride (MgCl) (25 mmol/L), 6 μL ddH₂O, and 1 μL DNA Master SYBR Green I (Roche). Either 1 μL of the external standard or 1 μL of complementary DNA were used as templates. PCR conditions were as follows: initial denaturation at 95°C for 30 seconds followed by 40 to 45 cycles including denaturation at 95°C for 1 second; annealing, *β-actin* at 60°C, *hMTH1* at 60°C, *hOGG1* at 64°C, *hMYHα* at 65°C, *MnSOD* at 62°C, for 3 seconds; and strand extension at 72°C for 30, 15, 15, 20, and 16 seconds, respectively. Total *hMYHα* values were calculated as the sum of mRNA expression levels of only subtypes *hMYHα3* and *hMYHα4*, as subtypes *hMYHα1* and *hMYHα2* were not expressed in liver tissue. The acquisition temperatures obtained via melting curve analysis were 87°C for *hMTH1*, 86°C for *hOGG1*, 87°C for *hMYHα*, 83°C for *MnSOD*, and 87°C for *β-actin*. The expression of all gene products was analyzed in relation to the housekeeping gene *β-actin* and multiplied by a factor of 100.

Cloning and Nucleotide Sequencing. All reverse transcription PCR products were cloned into the pST-Blue-1 AccepTor Vector (Novagen, Madison, WI) by means of the T-A cloning technique and sequenced (SeqLab, Göttingen, Germany).

Statistical Analysis. Data are expressed as median, range or percentage. Wilcoxon signed rank test was used for paired data. Unpaired groups were compared by Mann-Whitney and Kruskal-Wallis test as appropriate. Correlations between two variables were examined by Spearman rank correlation coefficient. A *P* value less than .05 was considered as statistically significant. Statistical

Table 2. Markers of Oxidative Damage and Hepatic Iron Content in tu and ntu Tissue

Patient No.	8-oxo-dG fmol/ μg DNA		MDA nmol/mg protein		Hepatic Iron mg/kg tissue dry weight	
	tu	ntu	tu	ntu	tu	ntu
1	37	33	0.13	0.11	89	994
2	22	27	0.53	0.40	39	85
3	16	75	0.15	1.20	171	1530
4	90	47			509	1140
5	56	53	0.60	0.66	258	1760
6	49	50	0.56	1.13	632	1440
7	59	133	0.31	0.47	389	13
8	20	46	0.70	0.94	337	1840
9	30	75	0.40	0.41	97	473
10	46	76			206	652
11	40	133	0.19	0.63	190	525
12	45	111	0.70	0.76	75	1070
13	58	387	0.78	3.77	2100	1610
14	27	129	0.10	0.17	95	26
15	25	141	0.45	0.30	37	82
16	113	144	0.83	1.34	116	209
17	72	226	0.33	1.04	84	817
18	52	136	0.78	1.09	22	224
19	115	91	0.74	1.27	97	91
20	134	248	0.42	1.50	344	947
21	361	220	0.59	0.61	705	1160
22	86	262	0.16	0.52	113	575
23	93	143			316	881
Median	52	129*	0.49	0.71*	171	817*

*P values (<.01) were derived by the Wilcoxon signed rank test.

analysis was performed with SPSS for Windows version 9.0 (Chicago, IL).

Results

Hepatic 8-oxo-dG Concentration and Inflammatory Activity. The median 8-oxo-dG concentration in ntu tissue was significantly ($P = .003$) higher than in tu tissue (Table 2). The different concentrations of 8-oxo-dG adducts in tu and ntu liver tissue were closely associated with the presence of inflammatory infiltration. Only 4 of 23 ntu tissues (17.4%) lacked significant inflammation, 13 (57.5%) revealed mild and 6 (26.1%) exhibited moderate inflammatory lymphohistiocytic infiltration. Overall, a trend for higher 8-oxo-dG concentration in ntu tissues with increased inflammatory infiltration ($P = .067$) was seen. Subgroup analysis revealed a significantly ($P = .02$) higher 8-oxo-dG concentration in ntu tissues with moderate inflammatory infiltration as compared to those with absent or mild inflammatory activity (Table 3). There was no relevant inflammatory activity in any of the tumor samples. Five (21.7%) tu tissues were graded as well differentiated (G1), 7 (30.4%) as moderately differentiated (G2), 4 (17.4%) as moderately to poorly (G2-G3) differentiated, and 7

(30.4%) as poorly differentiated (G3) carcinomas. There was no correlation between 8-oxo-dG concentration and tumor grade.

Hepatic Iron Concentration. In 17 of 23 patients (73.9%), the hepatic iron concentration was at least 2-fold higher in ntu tissues than in the corresponding tu samples (Table 2). The median iron content in ntu tissues was significantly ($P = .001$) higher than in tu tissues (Table 2). In the ntu tissue of 5 patients (21.7%), the hepatic iron concentration was above 1400 mg/kg tissue dry weight. Statistical analysis revealed no positive correlation of hepatic iron content and 8-oxo-dG concentration. In ntu tissues with moderate inflammatory infiltration, the hepatic iron content was significantly ($P = .036$) lower as compared to those with absent or mild inflammatory activity (Table 3).

Hepatic Lipid Peroxidation. Median MDA levels detected in HCCs were significantly ($P = .001$) lower than in the corresponding ntu tissue (Table 2). In ntu tissue, there was no association between MDA levels and grade of inflammatory infiltration (Table 3). There was

Table 3. Association of Markers of Oxidative Damage and Hepatic Iron Content in ntu Tissue With Inflammatory Infiltration

Patient No.	8-oxo-dG fmol/μg DNA		MDA nmol/mg protein		Hepatic Iron mg/kg tissue dry weight	
	0/+*	++*	0/+*	++*	0/+*	++*
1	33		0.11		994	
2	27		0.40		85	
3	75		1.20		1530	
4	47				1140	
5	53		0.66		1760	
6	50		1.13		1440	
7		133		0.47		13
8	46		0.94		1840	
9	75		0.41		473	
10	76				652	
11	133		0.63		525	
12	111		0.76		1070	
13	387		3.77		1610	
14		129		0.17		26
15		141		0.30		82
16	144		1.34		209	
17		226		1.04		817
18	136		1.09		224	
19	91		1.27		91	
20		248		1.50		947
21	220		0.61		1160	
22		262		0.52		575
23	143				881	
Median	76	183.3†	0.85	0.5	994	328†

*Grade of inflammatory infiltration: 0, absent or minimal; +, mild; ++, moderate.

†P values (<.05) were derived by the Mann-Whitney test.

no association between MDA levels and either 8-oxo-dG content or iron concentration in ntu or tu tissues.

Capacity of the Antioxidative Defence System. The GSH content was not significantly different between tu (median, 0.99; range, 0.19-5.13 $\mu\text{mol/g}$ tissue wet weight) and ntu tissues (median, 1.55; range, 0.42-5.26 $\mu\text{mol/g}$ tissue wet weight). No correlation was found between GSH content and 8-oxo-dG concentration, MDA levels, and iron concentration in tu and ntu tissues. The median GSH-Px activity was 60.5 U/g protein (range, 9.8-161 U/g protein) in tu, and 81 U/g protein (range, 4-205.7 U/g protein) in ntu, which was not significantly different. GSH-Px activity and GSH levels were negatively correlated in ntu tissue of the same patient ($r = -0.56$, $P = .009$). Expression of MnSOD mRNA was not significantly different between tu (median, 0.186; range, 0.010-1.257 *MnSOD*/ β -actin mRNA $\times 100$) and ntu tissues (median, 0.190; range 0.114-1.114 *MnSOD*/ β -actin mRNA $\times 100$).

Nuclear p53 Accumulation. Nuclear p53 protein accumulation was detectable in 6 of 21 tu tissues (28.6%) whereas this was not found in any ntu tissue. Only poorly ($n = 4$) or moderately to poorly ($n = 2$) differentiated HCCs showed nuclear accumulation of the p53 protein. There was no association with the extent of 8-oxo-dG formation.

***hMTH1*, *hOGG1* and *hMYH α* mRNA Expression.** A representative ethidium bromide-stained gel with *hMTH1*-, *hOGG1*-, *hMYH α* -, and β -actin-specific PCR products is shown in Figure 1. *hMYH α* revealed two amplicons that represent the hepatic *hMYH α 3* (upper band) and *hMYH α 4* (lower band) forms as confirmed by sequencing. In HCCs, the median *hMTH1* mRNA expression was 0.476 *hMTH1*/ β -actin mRNA $\times 100$ (range, 0.082-4.861 *hMTH1*/ β -actin mRNA $\times 100$), which was significantly ($P = .014$) higher than in ntu tissues (0.256; range 0.062-1.917 *hMTH1*/ β -actin mRNA $\times 100$) (Fig. 2A). In contrast, the median *hMYH α* mRNA expression (0.857; range, 0.092-8.152 *hMYH α* / β -actin mRNA $\times 100$) was significantly ($P = .039$) higher in ntu tissues than in HCC (0.424; range, 0.069-4.390 *hMYH α* / β -actin mRNA $\times 100$) (Fig. 2B). *hMYH α* mRNA expression was significantly correlated to *hMTH1* mRNA expression in ntu ($r = 0.497$, $P = .022$) (Fig. 3A) and in tu tissues ($r = 0.803$, $P < 0.001$) (Fig. 3B). No difference was seen for *hOGG1* mRNA expression in ntu (median, 1.256; range, 0.392-5.782 *hOGG1*/ β -actin mRNA $\times 100$) compared to tu tissues (median, 1.196; range, 0.370-6.687 *hOGG1*/ β -actin mRNA $\times 100$). *hOGG1* mRNA expression was significantly correlated to *hMTH1* mRNA expression in ntu ($r = 0.735$, $P < 0.001$) (Fig. 3C) and in tu tissues ($r = 0.86$, $P < 0.001$) (Fig. 3D).

Additionally, a positive correlation between *hOGG1* and *hMYH α* mRNA expression was found in ntu ($r = 0.535$, $P = .012$) (Fig. 3E) and in tu tissues ($r = 0.81$, $P < 0.001$) (Fig. 3F). There was no association between levels of *hMTH1*, *hOGG1*, and *hMYH α* mRNA expression and either 8-oxo-dG concentration, the extent of inflammatory infiltration, tumor grade, or p53 protein accumulation.

Discussion

Mice transgenic for the large hepatitis B surface gene exhibited increased production of ROS and elevated levels of 8-oxo-dG in their livers as compared to the non-transgenic control strain.²⁸ These animals develop chronic necroinflammatory liver disease that progresses to preneoplastic foci and eventually to HCC. Hagen et al. hypothesized that ROS production in activated Kupffer cells may have caused oxidative DNA damage in regenerating hepatocytes. 8-oxo-dG was observed by immunohistochemical labeling in patients with various forms of chronic liver diseases, and the number of stained hepatocytes was positively correlated to the severity of chronic hepatitis.²⁹ In a pilot study, Shimoda et al.³⁰ reported that the 8-oxo-dG content in liver samples of patients with chronic active hepatitis (but not in HCC) was significantly higher than in individuals without liver disease. In our study, we demonstrated that the 8-oxo-dG concentration in ntu liver tissues is significantly higher than in the corresponding HCC of the same subject (Table 2). In ntu tissue of patients with HCC, inflammatory infiltration to a various extent in dependence on the etiology is frequently seen.³¹ We found that 8-oxo-dG levels are significantly higher in ntu tissues with moderate inflammation compared to those with absent or mild inflammation (Table 3). Accordingly, Shimoda et al.³⁰ established a positive correlation between 8-oxo-dG concentration in ntu liver tissue and serum alanine aminotransferase activity. Increased 8-oxo-dG concentrations in ntu tissue of HCC patients compared to tu tissue and to ntu tissue of patients with primary non-HCC liver tumors or liver metastasis have been recently demonstrated.³² However, in contrast to our study, tu and ntu tissues were often not derived from the same patient. The higher median 8-oxo-dG levels measured in our study compared to these reports^{30,32} and to the study of Kato et al.³³ are most likely related to differences of methodology. Several variations of 8-oxo-dG levels have been reported, depending on the DNA extraction procedures and detection methods used.³⁴ Therefore, a comparison of absolute 8-oxo-dG values between different studies can be done only with caution, whereas a comparative analysis within a definite cohort in which the same methodology was used is appro-

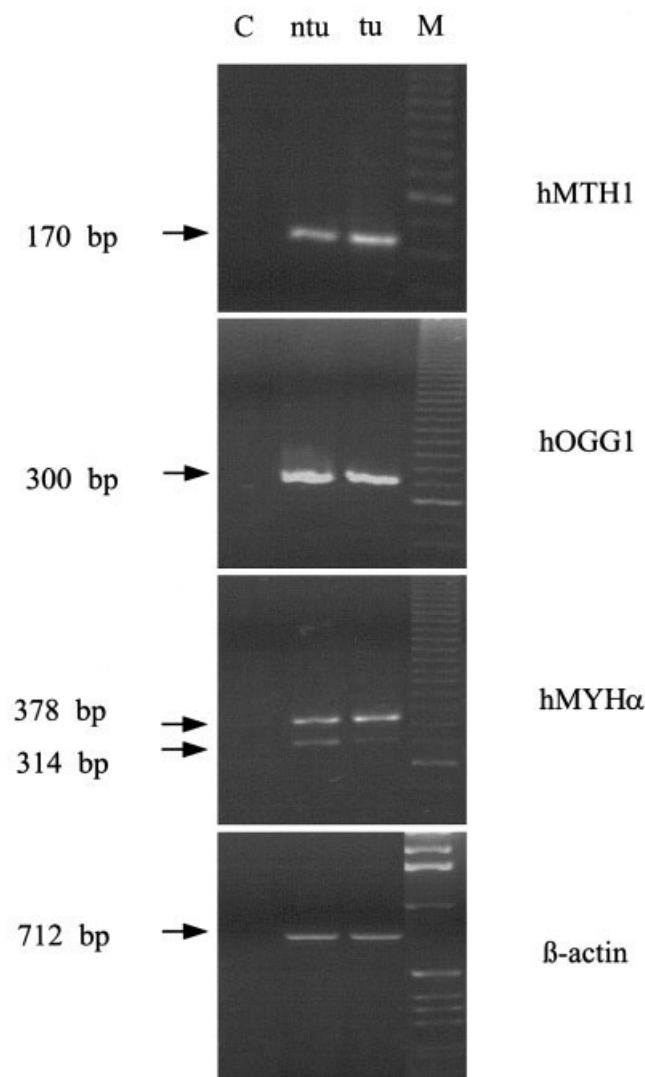


Fig. 1. Agarose gel electrophoresis of hepatic *hMTH1*, *hOGG1*, *hMYHα*, and β -actin amplicons after semiquantitative real-time reverse transcription polymerase chain reaction analysis. The fragment size of complementary DNA amplicons is given. bp, base pairs; C, negative control; M, size marker; ntu, nontumor; tu, tumor.

appropriate. The lack of a significant inflammatory infiltrate in our HCCs, in accordance with the typically low inflammatory infiltration in HCCs,³⁵ may explain their lower content of 8-oxo-dG. Furthermore, DNA adducts may have been diminished by DNA replication during rapid tumor cell turnover. Our results strengthen the hypothesis that chronic inflammation of the liver produces oxidative DNA damage that may increase the risk for genomic alterations.

Significantly higher hepatic 8-oxo-dG levels have been reported in iron-fed rats as compared to control groups.³⁶ Patients with hereditary hemochromatosis and cirrhosis have an increased risk for developing HCC; this may be due to iron-induced oxidative damage to DNA. In addition to the toxicity of excessive hepatic iron overload,

there is growing evidence that only mildly increased or even normal amounts of iron can serve as a cofactor in chronic liver disease.³⁷ Kato et al.³³ reported elevated 8-oxo-dG levels and iron overload in 34 patients with chronic HCV infection. The adduct levels significantly decreased to near normal levels after iron reduction therapy by phlebotomy. None of these patients developed HCC; however 1 out of 8 patients without phlebotomy did develop HCC. In our study, the median iron content in ntu tissues was approximately 5-fold higher than in tu tissues (Table 2). However, only 5 out of 23 patients exhibited mild hepatic iron overload in ntu tissues; therefore, increased "free" iron due to excessive iron overload

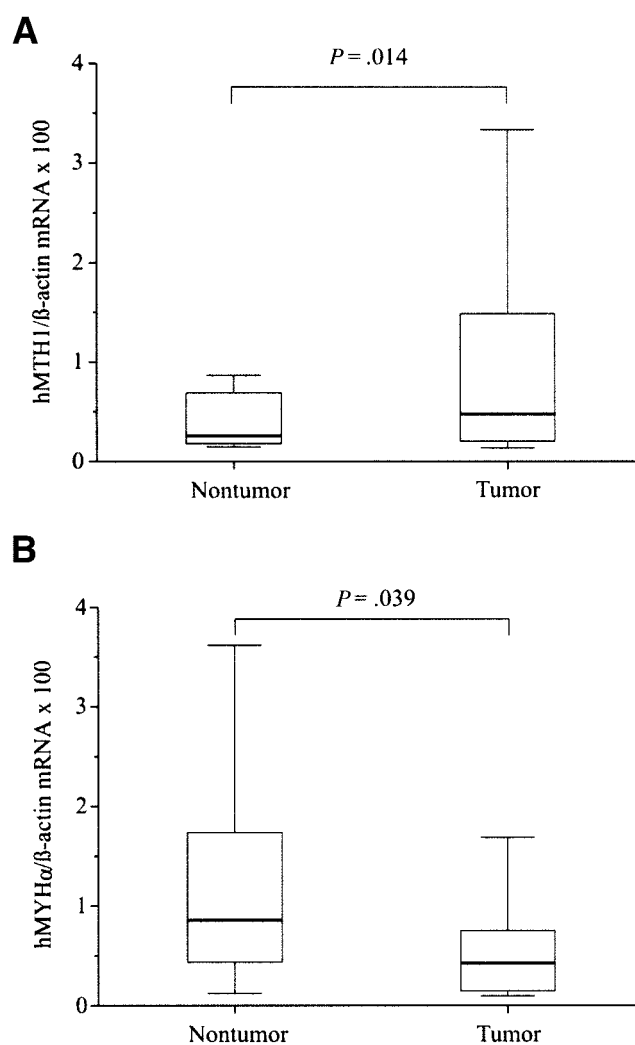


Fig. 2. Expression levels of DNA repair enzymes in tu and corresponding ntu tissue. Box-plot analysis of hepatic (A) *hMTH1* and (B) *hMYHα* messenger RNA expression in tumor and corresponding nontumor tissues using β -actin as an endogenous control for semiquantitative evaluation ($n = 21$). Median values are shown by the bold horizontal line, the box comprises values between the 25th and 75th percentiles, and the lower and upper bars indicate the 10th and 90th percentiles, respectively. The P value of the Wilcoxon signed rank test is given (P). mRNA, messenger RNA.

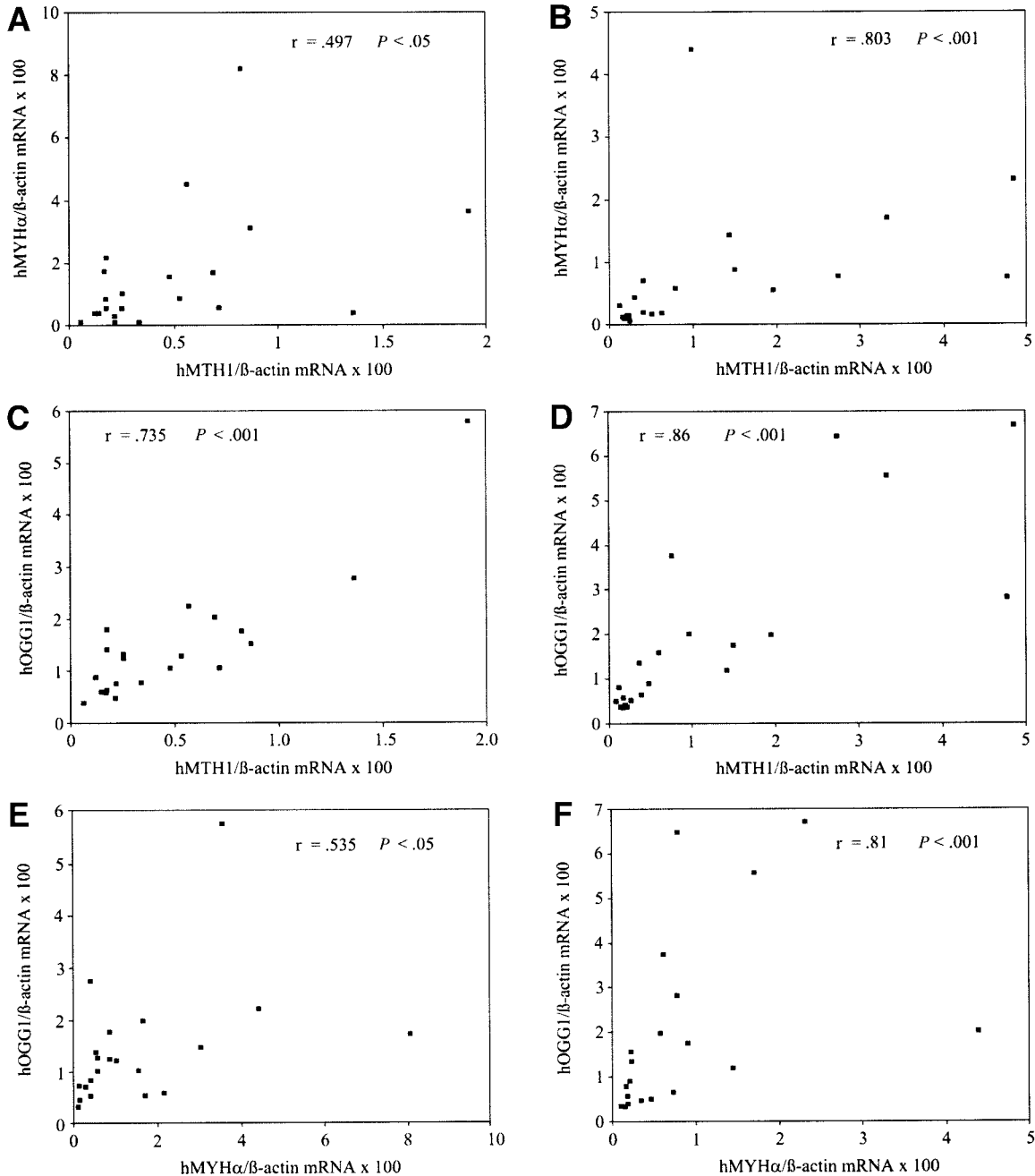


Fig. 3. Relationship between the messenger RNA (mRNA) expression of DNA repair enzymes in tu and corresponding ntu tissue. The correlation of *hMTH1* and *hMYHα* mRNA expression in (A) nontumor and (B) tumor tissues, *hMTH1* and *hOGG1* mRNA expression in (C) nontumor and (D) tumor tissues and *hOGG1* and *hMYHα* mRNA expression in (E) nontumor and (F) tumor tissues is shown. Correlation between two variables was calculated by Spearman rank correlation coefficient (r).

did not play a role. This may explain that there was no positive correlation between hepatic iron content and 8-oxo-dG concentration. Independent of the total hepatic iron content, increased “free” catalytic iron may occur in liver tissue with enhanced inflammatory infiltration, as ROS are known to release “free” iron from heme-containing compounds, iron storage proteins, and proteins containing iron-sulfur clusters.³⁸ Thus, iron may

be involved in oxidative damage (even in hepatic tissue without iron overload) and act as a cofactor in hepatic inflammatory disease.

Lipid peroxidation results in altered membrane function and production of toxic and reactive aldehydes, mainly MDA, which is capable of interacting with proteins or DNA and thereby may promote mutagenesis.^{6,8} These mechanisms may also be relevant for our patient

collective, as we detected significantly higher MDA levels in ntu tissue than in tu tissue (Table 2). In previous studies, decreased lipid peroxidation has been found in rat hepatoma tissues as compared to nonmalignant counterparts and in regenerating rat liver after partial hepatectomy.⁸ Therefore, it is still unclear whether increased resistance to lipid peroxidation is typical for cancer cells or whether it is a common feature of rapidly dividing cells.

GSH inhibited 8-oxo-dG formation *in vitro*³⁹ and was negatively correlated to 8-oxo-dG concentration in human lymphocytes.⁴⁰ In HCV core-transgenic mice that subsequently develop HCC, especially older animals showed increased levels of hepatic hydroperoxides of phosphatidylcholine and phosphatidylethanolamine and a reduction in GSH content as compared to nontransgenic controls.⁴¹ HCV infection may alter the oxidant/antioxidant ratio and thereby facilitate the development of HCC. In human HCCs, findings regarding the antioxidative capacity were inconsistent.^{42,43} In our study, we assessed the content of reduced GSH, GSH-Px activity, and *MnSOD* mRNA expression. There was neither a significant difference of the median values between tu and ntu tissue nor a correlation with ROS-mediated damage to lipids (MDA) or DNA (8-oxo-dG). This may be explained by either a possible compensatory up-regulation of other antioxidative enzymes or efficient DNA repair.

Tsuzuki et al.⁴⁴ generated an *MTH1* knockout mouse, which developed a greater number of spontaneous tumors of the liver, lung, and stomach 18 months after birth. In the present study, *hMTH1* mRNA was overexpressed in HCC compared to ntu tissue. This finding is in accordance with reports of elevated *hMTH1* mRNA expression in SV-40 transformed nontumorigenic human bronchial epithelial cells in 11 out of 12 human lung cancer cell lines⁴⁵ and in renal cell carcinomas.¹⁷ In these studies, 8-oxo-dG levels were also lower in transformed and malignant cells compared to normal controls. Effective removal of 8-oxo-dGTP by hMTH1 may, therefore, be an additional reason for the low 8-oxo-dG levels in HCCs. Up-regulation of *hMTH1* gene expression may be a reaction to a larger nucleotide precursor pool that is needed for DNA synthesis in proliferating tu cells.

An increase of *hOGG1* mRNA expression in human colorectal carcinoma tissues and a direct linear correlation with 8-oxo-dG levels has been reported previously.¹⁹ In human kidney tumors, no significant difference of *hOGG1* mRNA levels was found between normal and tumor tissues.¹⁸ A few homozygous mutations in the *hOGG1* gene were discovered in different types of cancer; some of these mutations may influence biochemical activity of the hOGG1 enzyme.¹⁸ In our study, the *hOGG1* mRNA expression was not significantly different between

HCC and ntu tissue. These data argue against an impact of hOGG1 in hepatocarcinogenesis; however, mutational inactivation of the *hOGG1* gene in some HCC cases cannot be ruled out. In ntu tissues, hOGG1 activity may be functionally inhibited by increased NO production in the inflammatory infiltrate, since NO mediated inhibition of hOGG1 activity has been shown in a cholangiocarcinoma cell line.⁴⁶ Studies with OGG1 knockout mice revealed an accumulation of elevated levels of 8-oxo-dG in liver tissue; however, only a moderate increase of the spontaneous mutation rate was observed, and no malignancies were detected.^{47,48} Possible reasons for these findings are limited fixation of mutations in slowly proliferating liver cells, repair of the opposite strand by a MutY homolog, or additional complementary repair functions of the nucleotide excision repair system. In our study, a highly significant positive correlation was obtained between the *hOGG1* and *hMTH1* mRNA expression in tu and ntu tissues, suggesting a cooperative action of these enzymes in the repair of 8-oxo-dG. Increased removal of the mispaired 8-oxo-dG via hOGG1 may result in augmentation of 8-oxo-dGTP in the nucleotide pool, resulting in up-regulation of *hMTH1* gene expression.

A significantly higher expression of *hMYHα* mRNA was detected in ntu tissue compared to tu tissue. *hMYHα* gene expression may have been up-regulated by high 8-oxo-dG concentrations and may represent a response to increased oxidative stress in ntu tissues to protect the integrity of cellular DNA. The significant positive correlation of *hMYHα* mRNA expression to *hMTH1* and *hOGG1* mRNA expression in tu and ntu tissues indicates that all three enzymes may act together to prevent 8-oxo-dG-induced mutagenesis. Mutated forms of hMYH protein, such as the nonconservative missense variants Tyr165Cys and Gly382Asp, were recently described in a single family that was affected by multiple colorectal adenomas and carcinomas.²⁰ The impact of similar sporadic mutations of the *hMYH* gene in HCC requires further investigation.

Diminished base excision repair has been reported in *p53* mutant and *p53*-null cells.¹² These cells exhibited very low activity of DNA polymerase beta, an enzyme required for base excision repair. We found that accumulation of the p53 protein in HCC, which is assumed to reflect p53 mutation, had no effect on the expression of cellular base excision repair genes *hOGG1* and *hMYH* at the mRNA level. Therefore, the p53 protein may not regulate these enzymes on a transcriptional level in human HCCs.

In conclusion, the results of our study indicate that inflammatory infiltration in ntu liver tissue of patients with HCC is closely linked to the occurrence of hepato-

cellular oxidative damage. In addition, hepatic iron may act as pro-oxidative cofactor. The DNA repair genes *hMTH1*, *hOGG1* and *hMYH* are differentially expressed at the mRNA level in tu and ntu tissue. Their role is likely to be more reactive to than causative for enhanced DNA damage. Unrepaired 8-oxo-dG adducts may initiate hepatocarcinogenesis. Our data thus provide an additional rationale for antioxidative and anti-inflammatory treatment, as shown for TJ-9 in a rat model⁴⁹ or interferon therapy in chronic hepatitis C patients,⁵⁰ to prevent HCC development.

Acknowledgment: This article is cordially dedicated to Professor Peter Hans Hofschneider, M.D., Ph.D., honorary D. at the occasion of his 75th birthday.

References

- Feitelson MA, Sun B, Satiroglu Tufan NL, Liu J, Pan J, Lian Z. Genetic mechanisms of hepatocarcinogenesis. *Oncogene* 2002;21:2593–2604.
- Wiseman H, Halliwell B. Damage to DNA by reactive oxygen and nitrogen species: Role in inflammatory disease and progression to cancer. *Biochem J* 1996;313:17–29.
- Kaplowitz N. Mechanisms of liver cell injury. *J Hepatol* 2000;32:39–47.
- Kasai H. Analysis of a form of oxidative DNA damage, 8-hydroxy-2'-deoxyguanosine, as a marker of cellular oxidative stress during carcinogenesis. *Mutat Res* 1997;387:147–163.
- Shibutani S, Takeshita M, Grollman AP. Insertion of specific bases during DNA synthesis past the oxidation-damaged base 8-oxodG. *Nature* 1991;349:431–434.
- Toyokuni S. Iron-induced carcinogenesis: The role of redox regulation. *Free Radic Biol Med* 1996;20:553–566.
- Deugnier Y, Turlin B, Loreal O. Iron and neoplasia. *J Hepatol* 1998;28:21–25.
- Cheeseman KH. Mechanisms and effects of lipid peroxidation. *Mol Aspects Med* 1993;14:191–197.
- Paradis V, Kollinger M, Fabre M, Holstege A, Poynard T, Bedossa P. In situ detection of lipid peroxidation by-products in chronic liver diseases. *HEPATOLOGY* 1997;26:135–142.
- Sun Y. Free radicals, antioxidant enzymes, and carcinogenesis. *Free Radic Biol Med* 1990;8:583–599.
- Vogelstein B, Kinzler KW. p53 function and dysfunction. *Cell* 1992;70:523–526.
- Seo YR, Fishel ML, Amundson S, Kelley MR, Smith ML. Implication of p53 in base excision DNA repair: in vivo evidence. *Oncogene* 2002;21:731–737.
- Furuichi M, Yoshida MC, Oda H, Tajiri T, Nakabeppu Y, Tsuzuki T, et al. Genomic structure and chromosome location of the human mutT homologue gene MTH1 encoding 8-oxo-dGTPase for prevention of A:T to C:G transversion. *Genomics* 1994;24:485–490.
- Aburatani H, Hippo Y, Ishida T, Takashima R, Matsuba C, Kodama T, et al. Cloning and characterization of mammalian 8-hydroxyguanine-specific DNA glycosylase/apurinic, apyrimidinic lyase, a functional mutM homologue. *Cancer Res* 1997;57:2151–2156.
- Slupska MM, Baikov C, Luther WM, Chiang JH, Wei YF, Miller JH. Cloning and sequencing a human homolog (hMYH) of the *Escherichia coli* mutY gene whose function is required for the repair of oxidative DNA damage. *J Bacteriol* 1996;178:3885–3892.
- Kennedy CH, Pass HI, Mitchell JB. Expression of human MutT homologue (hMTH1) protein in primary non-small-cell lung carcinomas and histologically normal surrounding tissue. *Free Radic Biol Med* 2003;34:1447–1457.
- Okamoto K, Toyokuni S, Kim WJ, Ogawa O, Kakehi Y, Arao S, et al. Overexpression of human mutT homologue gene messenger RNA in renal-cell carcinoma: Evidence of persistent oxidative stress in cancer. *Int J Cancer* 1996;65:437–441.
- Chevillard S, Radicella JP, Levalois C, Lebeau J, Poupon MF, Oudard S, et al. Mutations in OGG1, a gene involved in the repair of oxidative DNA damage, are found in human lung and kidney tumours. *Oncogene* 1998;16:3083–3086.
- Kondo S, Toyokuni S, Tanaka T, Hiai H, Onodera H, Kasai H, et al. Overexpression of the hOGG1 gene and high 8-hydroxy-2'-deoxyguanosine (8-OHdG) lyase activity in human colorectal carcinoma: regulation mechanism of the 8-OHdG level in DNA. *Clin Cancer Res* 2000;6:1394–1400.
- Al-Tassan N, Chmiel NH, Maynard J, Fleming N, Livingston AL, Williams GT, et al. Inherited variants of MYH associated with somatic G:C → A mutations in colorectal tumors. *Nat Genet* 2002;30:227–232.
- Desmet VJ, Gerber M, Hoofnagle JH, Manns M, Scheuer PJ. Classification of chronic hepatitis: Diagnosis, grading and staging. *HEPATOLOGY* 1994;19:1513–1520.
- Shigenaga MK, Aboujaoude EN, Chen Q, Ames BN. Assays of oxidative DNA damage biomarkers 8-oxo-2'-deoxyguanosine and 8-oxoguanine in nuclear DNA and biological fluids by high-performance liquid chromatography with electrochemical detection. *Methods Enzymol* 1994;234:16–33.
- Wong SH, Knight JA, Hopfer SM, Zaharia O, Leach CN Jr., Sunderman FW Jr. Lipoperoxides in plasma as measured by liquid-chromatographic separation of malondialdehyde-thiobarbituric acid adduct. *Clin Chem* 1987;33:214–220.
- Schramel P. Consideration of inductively coupled plasma spectroscopy for trace element analysis in the bio-medical and environmental fields. *Spectrochim Acta* 1983;38B:199–206.
- Sedlak J, Lindsay RH. Estimation of total, protein-bound, and nonprotein sulfhydryl groups in tissue with Ellman's reagent. *Anal Biochem* 1968;25:192–205.
- Paglia DE, Valentine WN. Studies on the quantitative and qualitative characterization of erythrocyte glutathione peroxidase. *J Lab Clin Med* 1967;70:158–169.
- Leifeld L, Cheng S, Ramakers J, Dumoulin FL, Trautwein C, Sauerbruch T, et al. Imbalanced intrahepatic expression of interleukin 12, interferon gamma, and interleukin 10 in fulminant hepatitis B. *HEPATOLOGY* 2002;36:1001–1008.
- Hagen TM, Huang S, Curnutte J, Fowler P, Martinez V, Wehr CM, et al. Extensive oxidative DNA damage in hepatocytes of transgenic mice with chronic active hepatitis destined to develop hepatocellular carcinoma. *Proc Natl Acad Sci U S A* 1994;91:12808–12812.
- Kitada T, Seki S, Iwai S, Yamada T, Sakaguchi H, Wakasa K. In situ detection of oxidative DNA damage, 8-hydroxydeoxyguanosine, in chronic human liver disease. *J Hepatol* 2001;35:613–618.
- Shimoda R, Nagashima M, Sakamoto M, Yamaguchi N, Hirohashi S, Yokota J, et al. Increased formation of oxidative DNA damage, 8-hydroxydeoxyguanosine, in human livers with chronic hepatitis. *Cancer Res* 1994;54:3171–3172.
- Kojiro M. Pathology of hepatocellular carcinoma. In: Okuda K, Tabor E, eds. *Liver Cancer*. Edinburgh: Churchill Livingstone; 1997:165–187.
- Schwarz KB, Kew M, Klein A, Abrams RA, Sitzmann J, Jones L, et al. Increased hepatic oxidative DNA damage in patients with hepatocellular carcinoma. *Dig Dis Sci* 2001;46:2173–2178.
- Kato J, Kobune M, Nakamura T, Kuroiwa G, Takada K, Takimoto R, et al. Normalization of elevated hepatic 8-hydroxy-2'-deoxyguanosine levels in chronic hepatitis C patients by phlebotomy and low iron diet. *Cancer Res* 2001;61:8697–8702.
- ESCOOD. Comparative analysis of baseline 8-oxo-7,8-dihydroguanine in mammalian cell DNA, by different methods in different laboratories: an approach to consensus. *Carcinogenesis* 2002;23:2129–2133.
- Ishak KG, Goodman ZD, Stocker JT. *Tumors of the liver and intrahepatic bile ducts*. Bethesda: Armed Forces Institute of Pathology; 2001:216.
- Kang JO, Jones C, Brothwell B. Toxicity associated with iron overload found in hemochromatosis: Possible mechanism in a rat model. *Clin Lab Sci* 1998;11:350–354.

37. Bonkovsky HL, Banner BF, Lambrecht RW, Rubin RB. Iron in liver diseases other than hemochromatosis. *Semin Liver Dis* 1996;16:65–82.
38. Keyer K, Imlay JA. Superoxide accelerates DNA damage by elevating free-iron levels. *Proc Natl Acad Sci U S A* 1996;93:13635–13640.
39. Spear N, Aust SD. Effects of glutathione on Fenton reagent-dependent radical production and DNA oxidation. *Arch Biochem Biophys* 1995;324:111–116.
40. Lenton KJ, Therriault H, Fulop T, Payette H, Wagner JR. Glutathione and ascorbate are negatively correlated with oxidative DNA damage in human lymphocytes. *Carcinogenesis* 1999;20:607–613.
41. Moriya K, Nakagawa K, Santa T, Shintani Y, Fujie H, Miyoshi H, et al. Oxidative stress in the absence of inflammation in a mouse model for hepatitis C virus-associated hepatocarcinogenesis. *Cancer Res* 2001;61:4365–4370.
42. Corrocher R, Casaril M, Bellisola G, Gabrielli GB, Nicoli N, Guidi GC, et al. Severe impairment of antioxidant system in human hepatoma. *Cancer* 1986;58:1658–1662.
43. Huang ZZ, Chen C, Zeng Z, Yang H, Oh J, Chen L, et al. Mechanism and significance of increased glutathione level in human hepatocellular carcinoma and liver regeneration. *Faseb J* 2001;15:19–21.
44. Tsuzuki T, Egashira A, Igarashi H, Iwakuma T, Nakatsuru Y, Tominaga Y, et al. Spontaneous tumorigenesis in mice defective in the MTH1 gene encoding 8-oxo-dGTPase. *Proc Natl Acad Sci U S A* 2001;98:11456–11461.
45. Kennedy CH, Cueto R, Belinsky SA, Lechner JF, Pryor WA. Overexpression of hMTH1 mRNA: a molecular marker of oxidative stress in lung cancer cells. *FEBS Lett* 1998;429:17–20.
46. Jaiswal M, LaRusso NF, Nishioka N, Nakabeppu Y, Gores GJ. Human Ogg1, a protein involved in the repair of 8-oxoguanine, is inhibited by nitric oxide. *Cancer Res* 2001;61:6388–6393.
47. Klungland A, Rosewell I, Hollenbach S, Larsen E, Daly G, Epe B, et al. Accumulation of premutagenic DNA lesions in mice defective in removal of oxidative base damage. *Proc Natl Acad Sci U S A* 1999;96:13300–13305.
48. Minowa O, Arai T, Hirano M, Monden Y, Nakai S, Fukuda M, et al. Mmh/Ogg1 gene inactivation results in accumulation of 8-hydroxyguanine in mice. *Proc Natl Acad Sci U S A* 2000;97:4156–4161.
49. Shiota G, Maeta Y, Mukoyama T, Yanagidani A, Udagawa A, Oyama K, et al. Effects of Sho-Saiko-to on hepatocarcinogenesis and 8-hydroxy-2'-deoxyguanosine formation. *HEPATOLOGY* 2002;35:1125–1133.
50. Camma C, Giunta M, Andreone P, Craxi A. Interferon and prevention of hepatocellular carcinoma in viral cirrhosis: An evidence-based approach. *J Hepatol* 2001;34:593–602.